ACS OMEGA

http://pubs.acs.org/journal/acsodf

Article

Kinetic Analysis of Laminar Combustion Characteristics of a H_2/Cl_2 Mixture at CO_2/N_2 Dilution

Jianing Chen, Guoyan Chen,* Weiwei Yu,* Anchao Zhang, Haoxin Deng, Xiaoping Wen, Fahui Wang, Yanyang Mei, and Wei Sheng

Cite This: *ACS Omega* 2022, 7, 7350−7360

Read Online

ACCESS | Metrics & More | Article Recommendations

ABSTRACT: Garbage and biomass contain more chlorine, which reacts with H_2 to form HCl gas during combustion or gasification, resulting in corrosion of metal walls. In this paper, based on the chlorine mechanism in Ansys Chemkin-Pro, the laminar combustion characteristics of H_2/Cl_2 are simulated with different diluents CO_2/N_2 under an initial temperature of 298 K, equivalence ratio range of 0.6−1.4, and initial pressure of 0.1−0.5 MPa. The results show that the laminar burning velocity of H_2/Cl_2 decreases significantly with the increase of dilution gas ratio, and the effect of diluent CO_2 is more significant than that of N_2. Due to the dilution effect, the fuel and oxidation components are reduced. Through sensitivity analysis, reaction R2: Cl + H_2 = HCl + H is the main reaction of HCl formation. On improving the initial pressure, the laminar burning velocity is slightly lowered, and the thermal diffusivity of the fuel mixture increases with the increase of the initial pressure. According to the sensitivity analysis of the velocity, reactions R2, R9, and R10 are the main reactions that affect the laminar burning velocity, and the product HCl will be generated with a delay with the increase of the initial pressure.

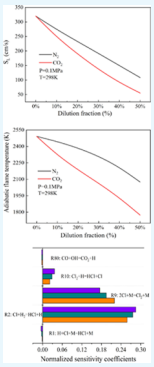

1. INTRODUCTION

Incineration is often used to treat liquid organic waste. As an essential part of hazardous liquid organic waste, chlorinated hydrocarbons have attracted considerable attention owing to their combustion characteristics.[1−7] Several studies have focused on hydrogen/chlorine flame.[8−15] Chlorine chemical fuels must be considered for solid combustion and gasification. We must consider both the emission of pollutants and the corrosiveness of chlorine.[16] Chlorinated hydrocarbons (e.g., chloromethane (CH_3Cl)), hydrogen chloride (HCl), or alkali chlorides (mainly KCl) are primarily used in the pyrolysis process of chlorine. During combustion, chlorine and hydrogen combine to produce a large amount of HCl. Because HCl is generally a product of chlorine in the combustion process, it is often removed in the fluidized bed combustion process.

Chlorine often affects the production of pollutants during combustion.[16] Generally, chlorine inhibits fuel oxidation.[17−21] However, chlorine is not as effective as other halogens.[22] Chlorine in fuel gas affects the formation of aromatic hydrocarbons and soot[23,24] as well as the emission of nitrogen oxides.[25] Additionally, chlorine affects the distribution of trace metals.[26,27] The high chlorine content can inhibit ignition,[28] reduce flame speed, and promote flame extinguishment. Rozlovskii,[29] Slootmaekers and Van Tiggelen,[8] and Corbeels and Scheller[14] experimentally measured the laminar combustion rate of hydrogen/chlorine. Recently, studies on flame theory and the experimental measurement of laminar combustion velocity have proved that Bunsen flame technology is affected by macrodynamic stretching effects,[30] particularly in the case of mixtures whose Lewis number (*Le*) deviates substantially from unity.

Chlorine constitutes a large proportion of most solid fuels (including coal and biomass).[31] The chlorine concentration in biomass fuels depends on the nutrient cycle and life parts of biomass materials. Generally, the chlorine content in wood is usually lower than that in coal, while the chlorine content in herbaceous biomass, fruits, and crops is considerably higher than that in coal.[32] Biomass, garbage, and other fuels contain a certain amount of chlorine. At present, in a combustion furnace of biomass power plants and garbage power plants, a certain amount of hydrogen will be formed due to the decomposition of water, and the combination of chlorine and hydrogen will form a certain amount of hydrogen chloride, which will strongly corrode the boiler and its tail flue. Therefore, studying the reaction of hydrogen and chlorine is of great significance for controlling the formation of hydrogen chloride in the furnace. In addition, the main components in the flue gas are N_2 and CO_2. These inert gases have a greater impact on the reaction of hydrogen and chlorine.

Only some studies have targeted the effect of diluents on the combustion characteristics of hydrogen/chlorine; however,

Received: December 27, 2021
Accepted: February 1, 2022
Published: February 15, 2022

diluents have different effects in our practical applications. Giurcan et al.[33−36] studied the influence of inert gas on fuel combustion characteristics. The laminar burning velocity has a vital influence on combustion characteristics and affects flame combustion stability. Thus, the effect of varying diluent contents on the hydrogen/chlorine laminar burning velocity was studied.

2. NUMERICAL CALCULATION

In this study, Ansys Chemkin-Pro was used to emulate the laminar flame characteristics of H_2/Cl_2 under different diluents. The PREMIX[37] and EQUIL[38] codes in the Chemkin package were used to emulate the free propagation of the laminar premixed flame of hydrogen and chlorine. This calculation used the chlorine chemical[39] reaction mechanism, which involved 102 reactions and 25 substances. To meet the calculation requirements and achieve zero gradients for all variables, an adaptive grid with a GRAD and CURV of 0.02 was used in the current simulation. The right and left sides of the calculation domain were 10 and −0.2 cm, respectively, and the number of grids was 1000. In the presence of hydrogen, the Soret effect and multicomponent transport model were deemed to determine the completely convergent flame velocity prediction in this simulation.

Table 1. Calculation Settings

variables	range
fuel	H_2
oxidant	Cl_2
initial temperature (T)	298 K
initial pressure (p)	0.1−0.5 MPa
diluent	N_2 and CO_2
fraction of diluent (μ)	0−50%
equivalence ratio	0.6−1.4

To evaluate the effect of diluents on H_2/Cl_2, different proportions of N_2/CO_2 were added to the mixture. The fuel diluent method[15,40] was used to determine the diluent concentration, in which μ% was the diluent content and $(100 - \mu)$% H_2 was burned in Cl_2.

$$\mu\% = \frac{n_{\text{diluent}}}{n_{\text{diluent}} + n_{H_2}} \quad (1)$$

where μ% represents the diluent content, n_{diluent} is the mole fraction of the diluent in the mixture, and n_{H_2} is the mole fraction of hydrogen in the mixture. Based on the existing work, the initial temperature and pressure were 298 K and 0.1−0.5 MPa, respectively, and the upper limit of the diluent proportion was 50%. Table 1 lists the initial calculation settings.

3. RESULTS AND DISCUSSION

3.1. Mechanism Verification. Studies on H_2/Cl_2 combustion are limited. In Figure 1, the experimental data in the literature[41] are compared with the simulation results. This figure indicates that the laminar burning velocity was satisfactory. We used the chlorine mechanism in the simulation calculation.

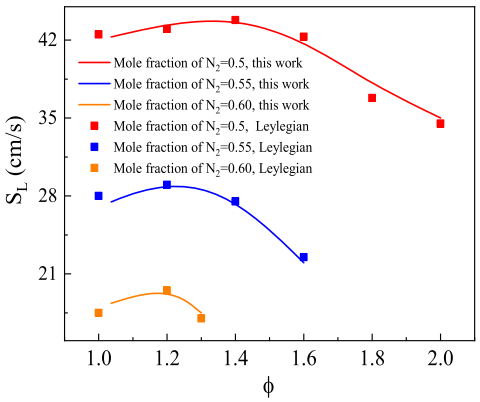

Figure 1. Comparison between the predicted LBVs and experimental data.

3.2. Effect of the Diluent Content on LBV and Adiabatic Flame Temperature. Laminar burning velocity (LBV) often describes the basic parameters of fuel reactivity, heat release, and thermal diffusivity. The adiabatic flame temperature (AFT) refers to the temperature at which the fuel can reach the equilibrium (or the highest temperature) without losing any heat under the same pressure.[42] Figure 2 presents an alternative distribution of the LBV and AFT for hydrogen and chlorine combustion under different diluents calculated using Ansys Chemkin-Pro. Additionally, STANJAN[43] was used to estimate the thermal diffusivity under various diluent ratios. As the diluent concentration increased (at the same equivalence ratio), the thermal diffusivity lessened considerably. The N_2 diluent showed a higher thermal diffusivity than the CO_2 diluent.

Moreover, the AFT increased remarkably when the equivalence ratios were 0.6−1.1, reaching a peak at ∼1.1. Then, the AFT decreased at equivalence ratios of 1.1−1.4 (Figure 2c,d). As the diluent proportion increased, the AFT decreased considerably. As a diluent, N_2 achieved a higher AFT than CO_2. In Figure 2a,b, to find the inflection point of the laminar burning velocity, we increased the equivalence ratio range. It can be clearly observed that when N_2 is used as the main diluent, the maximum laminar burning velocity appears at about 1.45 equivalence ratio. When CO_2 is used as the main diluent, the maximum laminar burning velocity appears at about 1.55 equivalence ratio. The N_2 diluent achieved a higher laminar burning velocity than the CO_2 diluent. According to laminar burning velocity theory,[44] $S_L \propto (\alpha \text{RR})1/2$, the laminar flame velocity is directly proportional to thermal diffusivity (α) and AFT (T_{ad}) and directly associated with the reaction rate (RR). In the process of H_2/Cl_2 combustion, the adiabatic flame temperature decreases when the equivalence ratio is 1.1, the thermal diffusivity increases as the equivalence ratio increases, and the laminar burning velocity changes trend similar to the thermal diffusivity. According to the above formula, in H_2/Cl_2 combustion, the thermal diffusivity has a greater influence on the laminar burning velocity than the adiabatic flame temperature. Based on a previous study, increasing the inert gas content will reduce the laminar burning velocity and the adiabatic flame temperature, which is due to the increase of thermal capacity and the change of thermal performance of hydrocarbon fuels.[30] Currently, the combustion of hydrogen and chlorine varies. Enhancing the inert gas content mainly reflected the dilution effect and decreased the fuel and oxidation components.

3.2.1. Sensitivity Analysis. To explore the influence of the concentration and type of diluents on the laminar burning

https://doi.org/10.1021/acsomega.1c07313
ACS Omega 2022, 7, 7350−7360

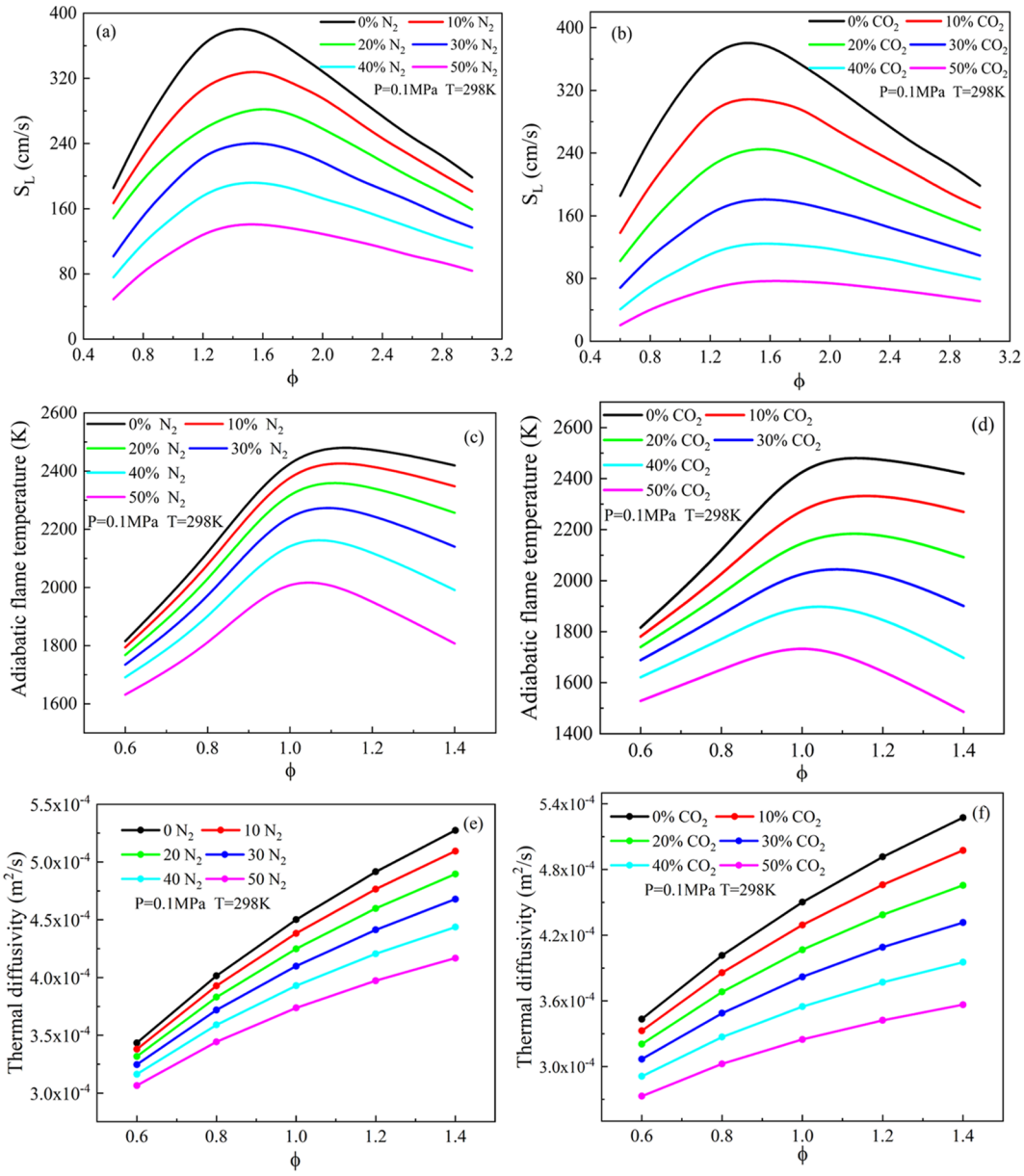

Figure 2. Mechanism validation: (a, b) laminar burning velocity, (c, d) adiabatic flame temperature, and (e, f) thermal diffusivity of $H_2/Cl_2/N_2/CO_2$ mixtures at different fuel compositions.

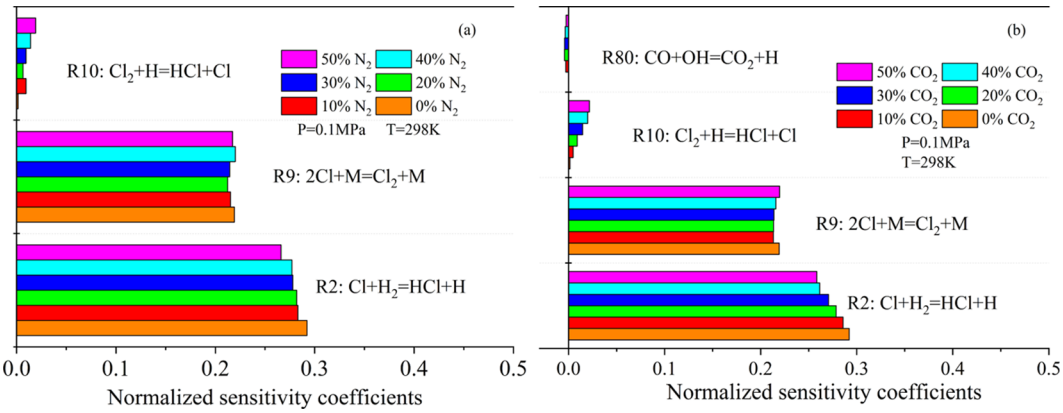

Figure 3. Sensitivity analysis of different $H_2/Cl_2/N_2/CO_2$ mixtures: (a) N_2 and (b) CO_2.

https://doi.org/10.1021/acsomega.1c07313
ACS Omega 2022, 7, 7350−7360

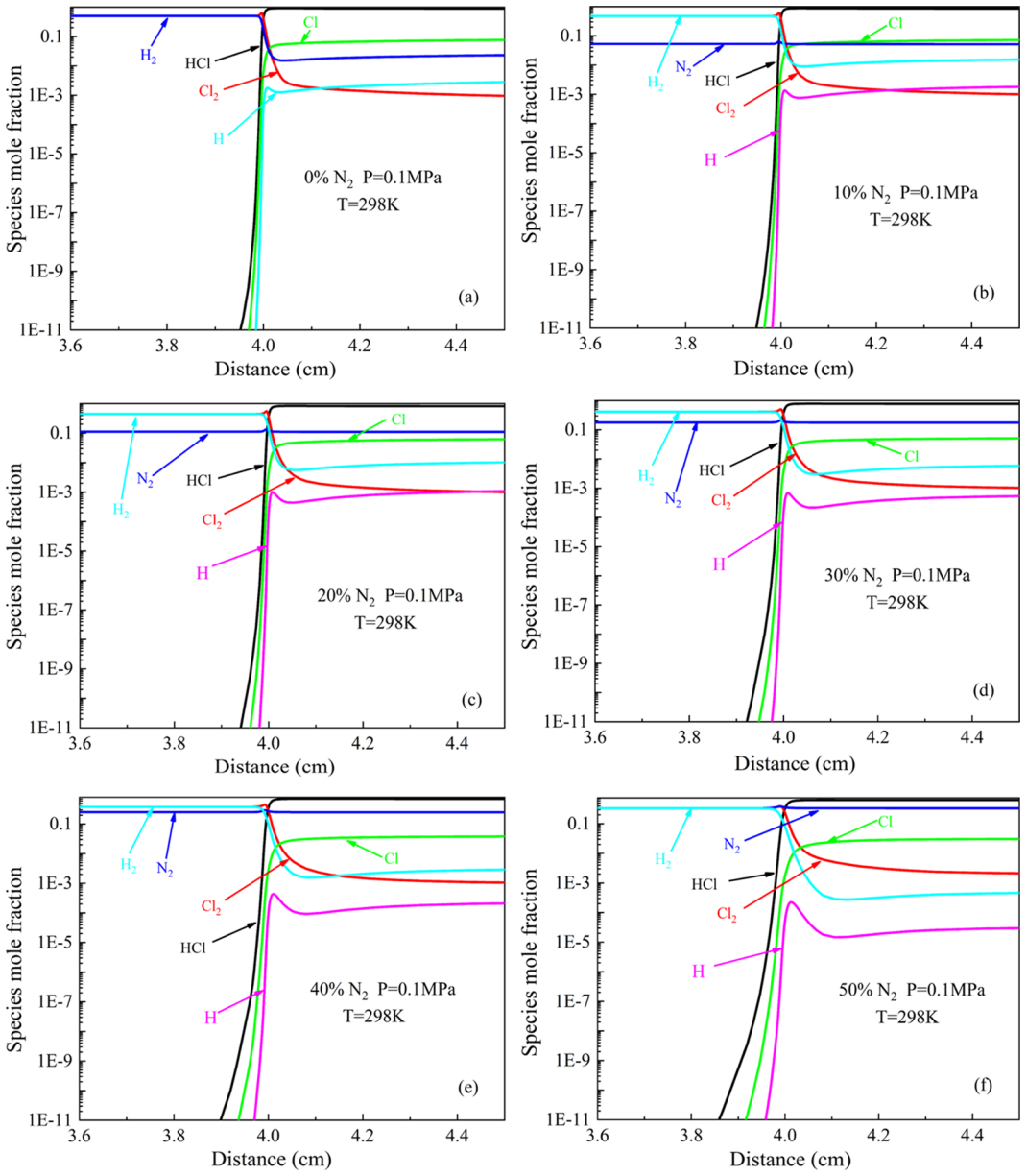

Figure 4. Mole fraction of $H_2/Cl_2/N_2$ flames at a temperature of T = 298 K and a pressure of P = 0.1 MPa: (a) 0% N_2, (b) 10% N_2, (c) 20% N_2, (d) 30% N_2, (e) 40% N_2, and (f) 50% N_2.

velocity, the normalized sensitivity coefficients were emulated using the PREMIX code in the Chemkin package. Figure 3 presents the normalized sensitivity coefficient of the diluents with respect to the laminar burning velocity of hydrogen and chlorine. When N_2 was used as the diluent, the primary reaction affecting the laminar burning velocity was R2: Cl + H_2 = HCl + H (Figure 3a); this reaction generated massive quantities of HCl and H. The second reaction was R9: 2Cl + M = Cl_2 + M, which produced large quantities of Cl_2. Another reaction R10: Cl_2 + H = HCl + Cl occurred, which had less impact; this reaction also generated HCl and Cl. Alternatively, when CO_2 was used as the diluent, reactions R2, R9, and R10 slightly differed from those in the case where N_2 was used as the diluent. Reaction R80: CO + OH = CO_2 + H inhibited the laminar burning velocity. Under diverse diluent concentrations, the influence of the laminar burning velocity also varied considerably. In the absence of a diluent, reactions R10 and R80 did not occur; however, the sensitivity coefficients of reactions R2 and R9 reached the maximum values. When the N_2 diluent content was increased, the sensitivity coefficient of reaction R2 decreased. Moreover, the sensitivity coefficient of reaction R9 first decreased, then increased, and subsequently decreased. The maximum sensitivity coefficient of reaction R9 was achieved at an N_2 content of 40%. Further, the sensitivity coefficient of reaction R10 increased as the content of the N_2 diluent increased. When the CO_2 diluent content was increased, the sensitivity coefficient of reaction R2 decreased, while the maximum sensitivity coefficient of R9 was achieved when the CO_2 content was 50%. Based on the sensitivity analysis of the laminar burning velocity, the contents of H_2, Cl, and H radicals were found to have the greatest influence on the laminar burning velocity.

3.2.2. Chemical Kinetic Structures. A numerical simulation was performed to study the detailed chemical kinetic structure of hydrogen and chlorine flame under different diluents using the chlorine mechanism. For each fuel composition, the

https://doi.org/10.1021/acsomega.1c07313
ACS Omega 2022, 7, 7350−7360

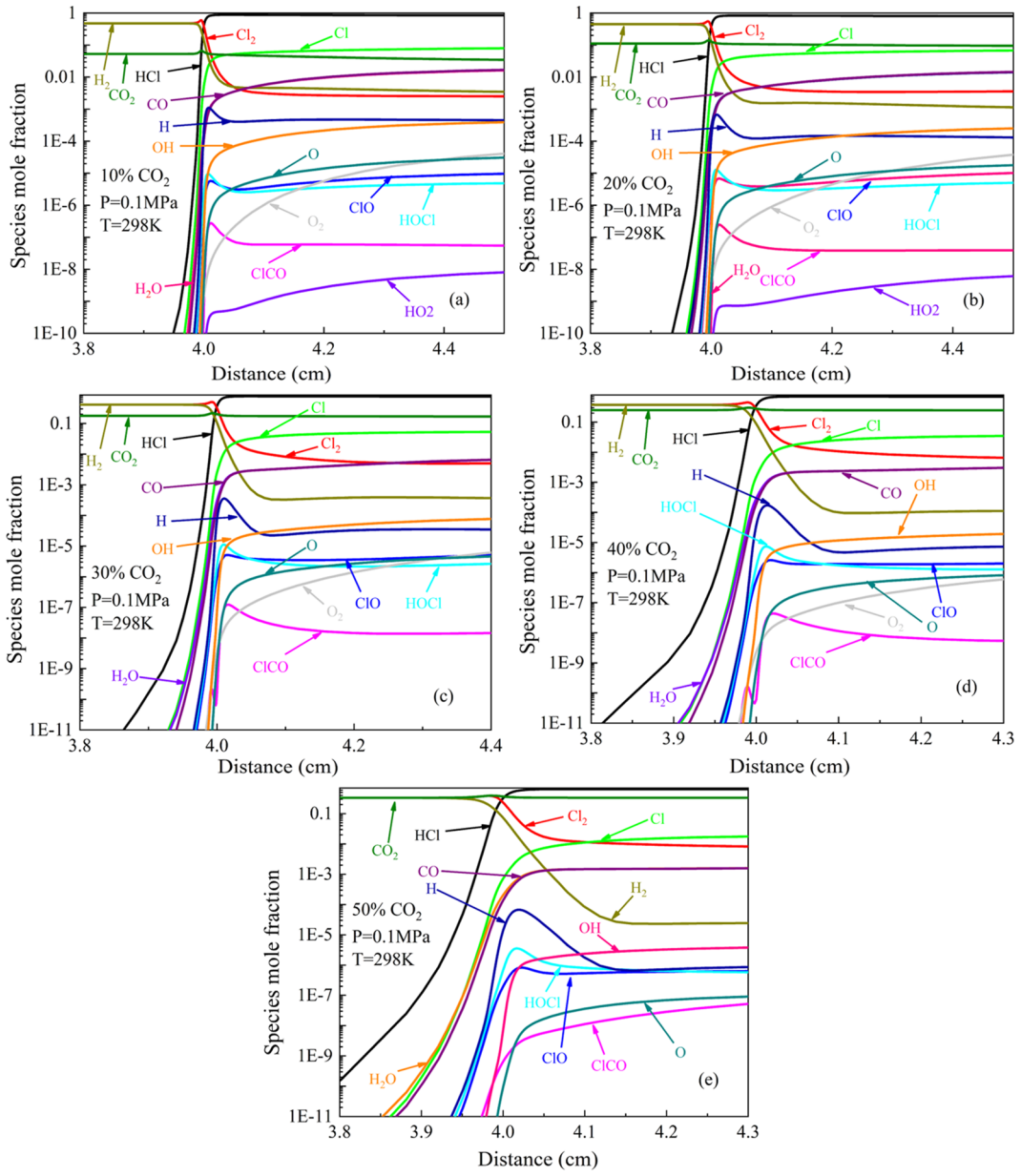

Figure 5. Mole fraction of $H_2/Cl_2/CO_2$ flames at a temperature of T = 298 K and a pressure of P = 0.1 MPa: (a) 10% CO_2, (b) 20% CO_2, (c) 30% CO_2, (d) 40% CO_2, and (e) 50% CO_2.

substance mole fraction, productivity, and net reaction rate were plotted as follows. First, when N_2 was used as the diluent, combustion mainly occurred at distances of 3.9−4.1 cm (Figure 4). During this period, massive quantities of HCl gas were generated. Moreover, the amount of chlorine gas increased slightly and then decreased sharply. The H content first increased, then decreased, and finally increased, which was associated with a decrease in the H_2 content, particularly, when the diluent concentration was high. N_2 also increased slightly and then decreased slightly. Figure 4c,d shows that the change in the mole fraction of N_2 is more obvious. With the increase of N_2, the molar fraction of the H radical decreases, which has a great influence on the laminar burning velocity. When CO_2 was used as the main diluent, the mole fraction of each substance became more complex. Figure 5 indicates that with increasing diluent content, the combustion advanced, which was more obvious when the CO_2 diluent content was 50%. Additionally, H_2O was formed before other substances. Perhaps, water inhibited the laminar burning velocity, implying that the laminar burning velocity of the N_2 diluent was greater than that of the CO_2 diluent. As the diluent content increased, the mole fractions of H and Cl radicals decreased. Consequently, an increase in the diluent content decreased the flame laminar burning velocity based on LBV sensitivity analysis. N_2 was used as the main diluent for the production of each substance (Figure 6). Clearly, with increasing diluent content, the production rate of each substance decreased but the combustion distance increased. Compared with the N_2 diluent, the production rate of each substance was lower when the same concentration of the CO_2 diluent was used; however, the combustion distance increased further (Figure 7). The overall trend was the same in the case of both diluents. Figure 8 shows the net reactions using the N_2 diluent, i.e., R2, R9, and R10. Overall, reactions R2 and R10 showed nearly the same

https://doi.org/10.1021/acsomega.1c07313
ACS Omega 2022, 7, 7350−7360

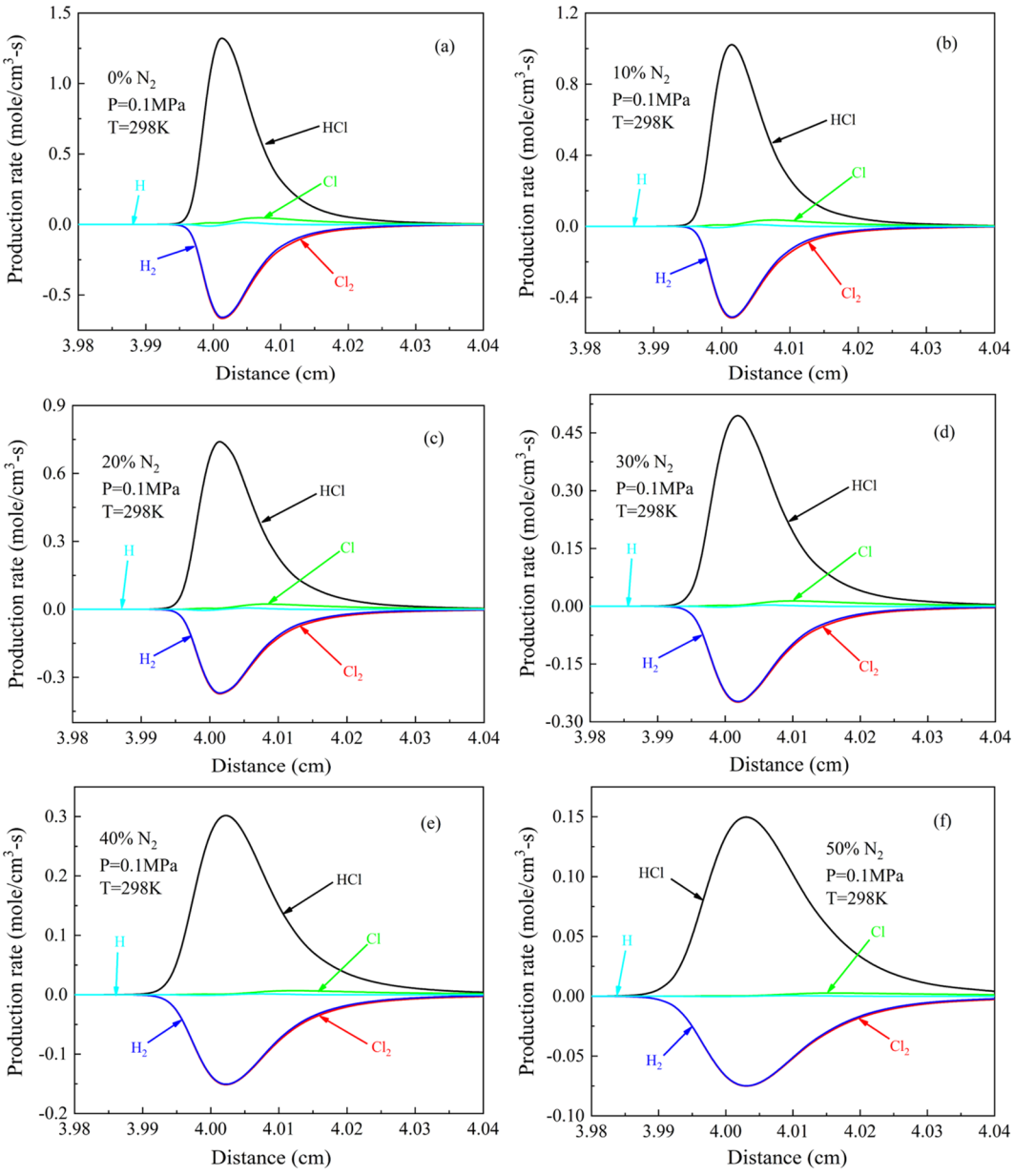

Figure 6. Production rates of $H_2/Cl_2/N_2$ flames at a temperature of T = 298 K and a pressure of P = 0.1 MPa: (a) 0% N_2, (b) 10% N_2, (c) 20% N_2, (d) 30% N_2, (e) 40% N_2, and (f) 50% N_2.

trends; both reactions initially increased and then decreased. A large amount of HCl was generated during this period; hence, reactions R2 and R10 were mainly responsible for generating HCl. R9 first decreased and then increased, during which a small amount of Cl_2 was produced, promoting reaction R10. With increasing N_2 diluent content, the net RR reduced considerably. At a N_2 content of 50%, the decrease in the net reaction rate was ~89%. Figure 9 shows that the overall trend of CO_2 was similar to that of N_2. The net reaction rate was lower when using CO_2 as the main diluent compared with when N_2 was used as the main diluent. Compared with N_2 diluent, CO_2 diluent increased R80: CO + OH = CO_2+H.

3.3. Effect of Pressure on the Laminar Burning Velocity. Figure 10 indicates the effect of diverse initial pressures (0.1, 0.3, and 0.5 MPa) and equivalence ratios on the laminar burning velocity of H_2/Cl_2 using a 50% CO_2/N_2 diluent. The laminar burning velocity decreased slightly with increasing initial pressure. Compared with hydrocarbon fuels, the laminar burning velocity change was not apparent. Because the thermal diffusivity of the fuel mixtures increased with increasing initial pressure, at higher pressures, the laminar burning velocity tended to have an equivalence ratio greater than about 1.4.[44] This observation is discussed in more detail in Sections 3.3.1−3.3.3.

3.3.1. Laminar Burning Flux. According to a study by Law and Sung,[30] the laminar burning flux, $f^0 = \rho_u s_L$, is the essential parameter of flame propagation. It mainly shows the reactivity, diffusivity, and exothermicity of the fuel mixture. Figure 11 presents the laminar burning flux of H_2/Cl_2 using the 50% CO_2/N_2 diluent under different initial pressures. As the initial pressure increases, the laminar burning flux increases and the laminar burning velocity decreases; this result is consistent with the conclusion obtained by Law.[45] Law reported that an increase in density induces a phenomenon, where the laminar burning velocity decreases with an increase in the initial pressure. Based on the research by Law et al.,[30] we know that

https://doi.org/10.1021/acsomega.1c07313
ACS Omega 2022, 7, 7350−7360

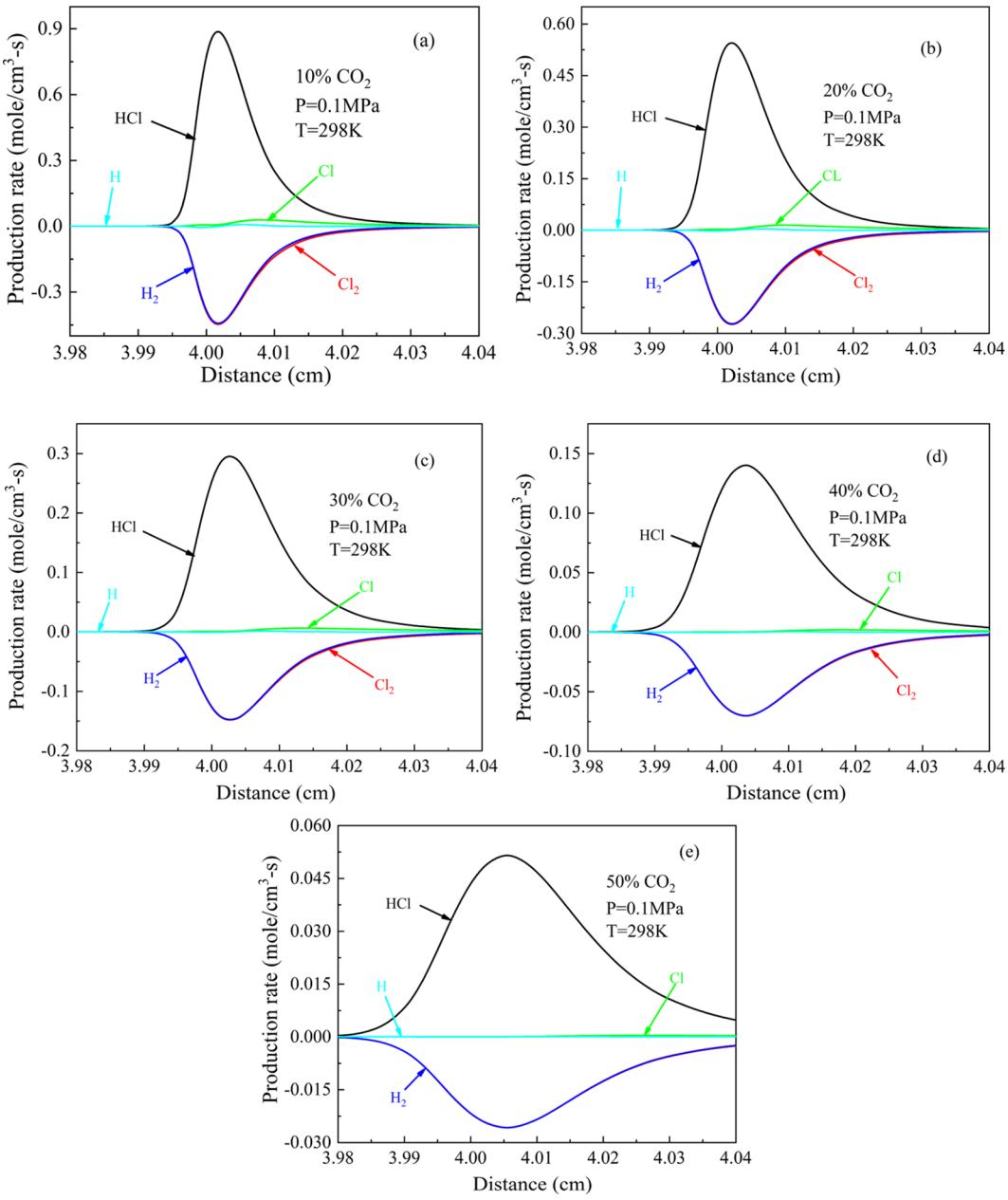

Figure 7. Production rates of $H_2/Cl_2/CO_2$ flames at a temperature of T = 298 K and a pressure of P = 0.1 MPa: (a) 10% CO_2, (b) 20% CO_2, (c) 30% CO_2, (d) 40% CO_2, and (e) 50% CO_2.

$S_b^0 \sim [(\lambda/c_P)_b w_b]^{1/2}/\rho_b$, indicating that laminar flame responses rely on the flame dynamics of the characteristic reaction rate w_b as well as transport processes based on the density-weighted transport coefficient $(\lambda/c_P)_b$. For the study, density is very important because it determines the meaning of the part of diffusive transport as well as that of the mass flow rate.[46]

3.3.2. Sensitivity Analysis. To study the most significant elemental reactions affecting the laminar burning velocity varying initial pressures, a sensitivity analysis was conducted on the laminar burning velocity of H_2/Cl_2 at different pressures using the 50% N_2/CO_2 diluent (Figure 12). When the initial pressure was increased, the number of collisions between molecules and free radicals increased and the reaction became more complex. The positive sensitivity coefficient of reactions R2 and R10 increased with a change in the initial pressure. This can be verified based on the increasing trend of the laminar burning flux, which increased with the initial pressure.[14] Conversely, reaction R9 decreased as the initial pressure increased. Generally, R2 was the primary reaction responsible for HCl formation. A previous related literature[47] revealed that as the initial pressure increased, the termination of the reaction became extremely critical. Therefore, the delay impact was assessed for the entire combustion reaction. Such end reactions could supersede the central part of the branching reaction, particularly in the case of three bodies, the rate of which increased considerably with increasing pressure.

3.3.3. Chemical Kinetic Research. Figure 13 shows that the different initial pressures changed for the H, Cl, and HCl mole fractions using the 50% CO_2/N_2 diluent. The formation of H, Cl, and HCl was delayed as the pressure increased. When the diluent was 50% N_2, the initial pressure of H radicals in equilibrium was 0.3 MPa, which was the maximum value.

https://doi.org/10.1021/acsomega.1c07313
ACS Omega 2022, 7, 7350−7360

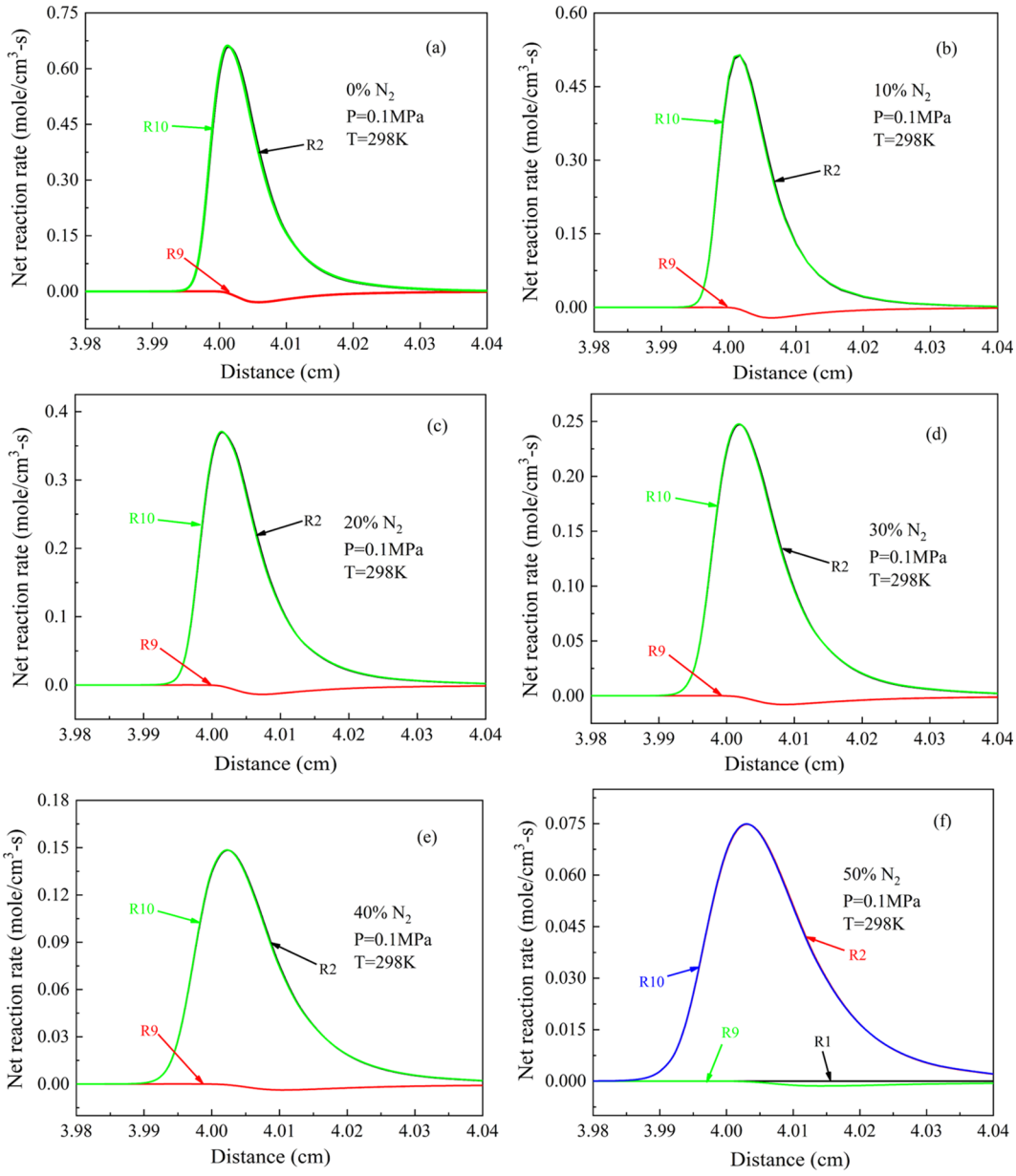

Figure 8. Net reaction rates of $H_2/Cl_2/N_2$ flames at a temperature of T = 298 K and a pressure of P = 0.1 MPa: (a) 0% N_2, (b) 10% N_2, (c) 20% N_2, (d) 30% N_2, (e) 40% N_2, and (f) 50% N_2.

Furthermore, the initial pressure of H radicals in equilibrium was 0.5 MPa when the diluent was 50% CO_2, which was the maximum value. The maximum mole fraction was observed at an initial pressure of 0.1 MPa when Cl and HCl were in equilibrium, signifying that the formation of the main product HCl was delayed with increasing initial pressure when H_2/Cl_2 was combusted.

4. CONCLUSIONS

Herein, Ansys Chemkin-Pro is used based on the chlorine mechanism to study the different combustion characteristics of H_2/Cl_2 under different diluents and initial pressures. The thermal diffusivity, laminar burning velocity, adiabatic flame temperature, free radicals, intermediate substances, and sensitivity analysis of velocity are analyzed.

(1) The maximum laminar burning velocity of H_2/Cl_2 is observed when the equivalent ratio is about 1.4. The laminar burning velocity and adiabatic flame temperature of the N_2 diluent are higher than those of the CO_2 diluent. H_2/Cl_2 combustion of the diluent is mainly the dilution effect, which reduces the fuel and oxidation components.

(2) Based on the sensitivity analysis of the laminar burning velocity, mainly for R2: Cl + H_2 = HCl + H and R9: 2Cl + M = Cl_2 + M, the contents of H_2, Cl, and H radicals are found to have the greatest influence on the laminar burning velocity. The addition of the CO_2 diluent makes the combustion more complicated, and numerous free radicals are generated, resulting in unstable combustion.

(3) The laminar burning velocity decreases slightly with an increase in the initial pressure, and the laminar burning flux increases with the initial pressure. The initial pressure increases, leading to the delayed production of the main product HCl.

https://doi.org/10.1021/acsomega.1c07313
ACS Omega 2022, 7, 7350−7360

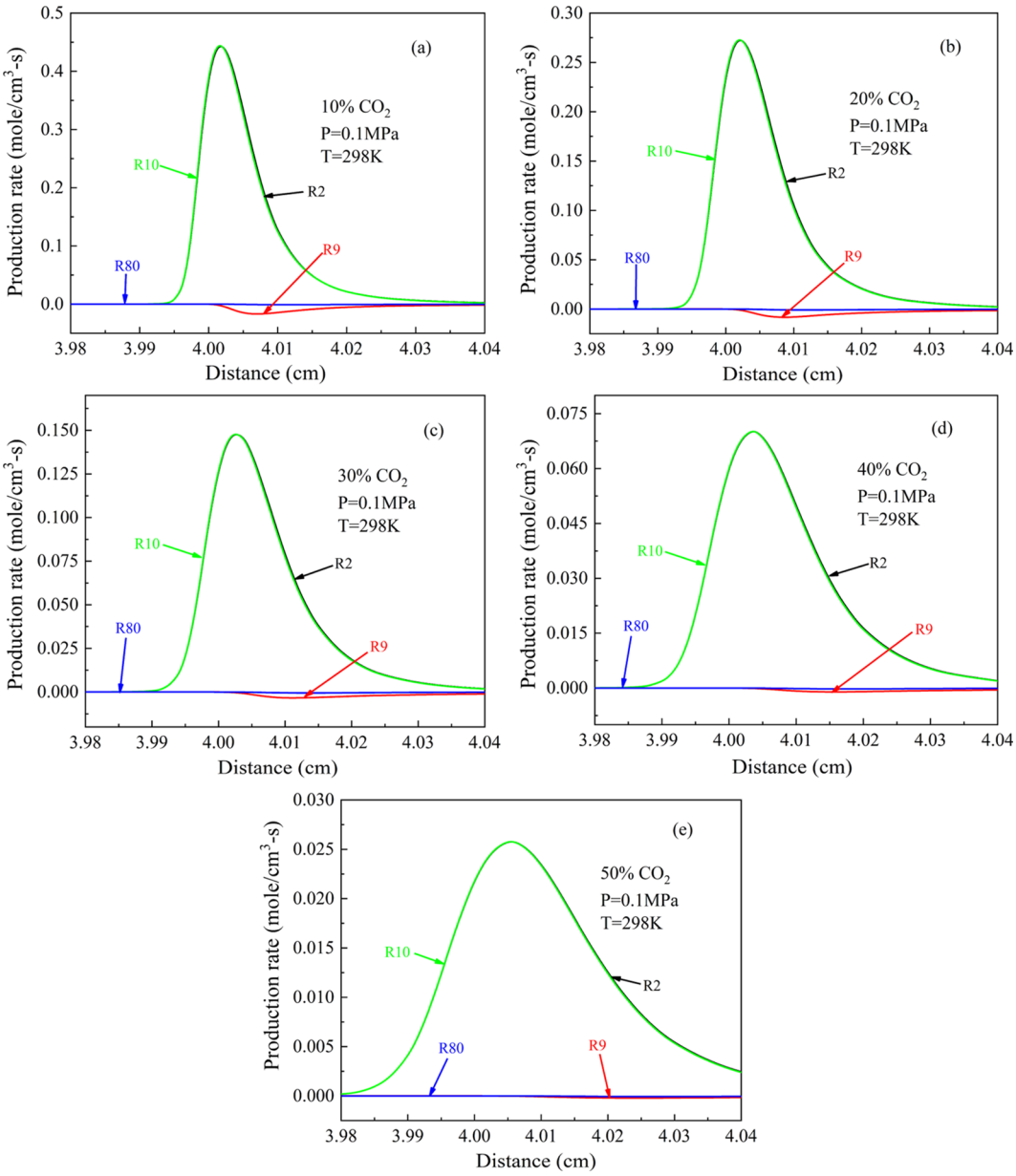

Figure 9. Net reaction rates of $H_2/Cl_2/CO_2$ flames at a temperature of T = 298 K and a pressure of P = 0.1 MPa: (a) 10% CO_2, (b) 20% CO_2, (c) 30% CO_2, (d) 40% CO_2, and (e) 50% CO_2.

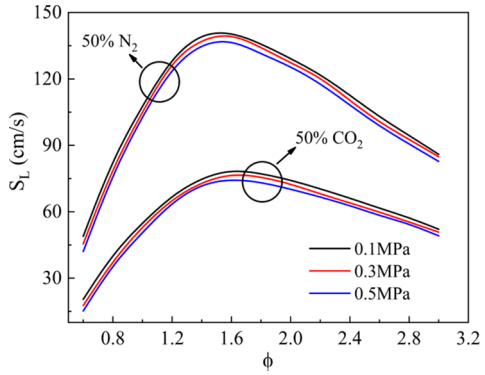

Figure 10. Laminar burning velocity of $H_2/Cl_2/N_2/CO_2$ at different initial pressures.

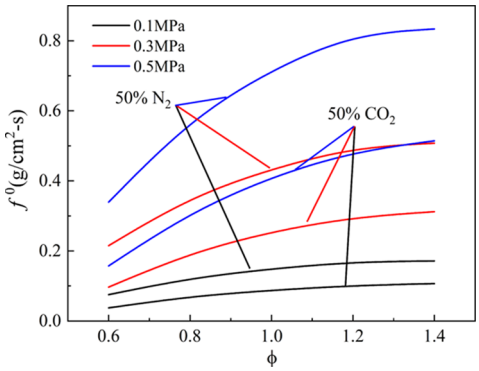

Figure 11. Laminar burning flux of $H_2/Cl_2/CO_2/N_2$ mixtures at different initial pressures.

https://doi.org/10.1021/acsomega.1c07313
ACS Omega 2022, 7, 7350−7360

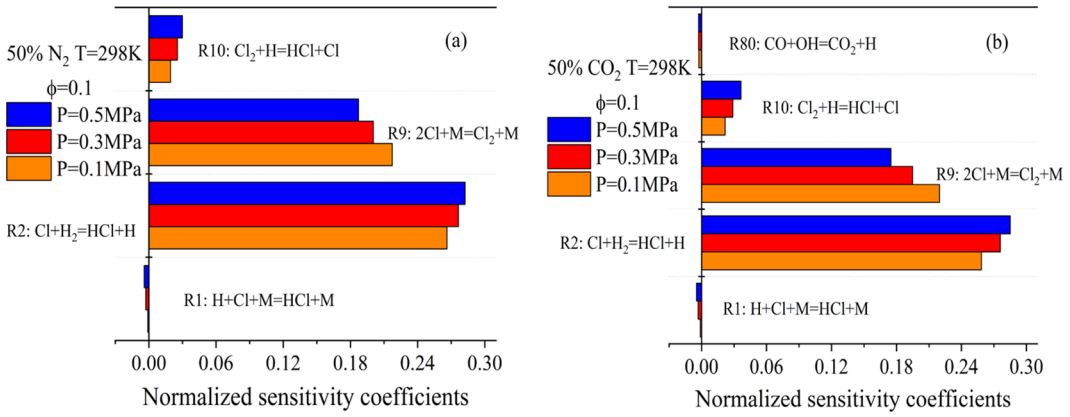

Figure 12. Sensitivity analysis of different premier pressures: (a) 50% N_2 and (b) 50% CO_2.

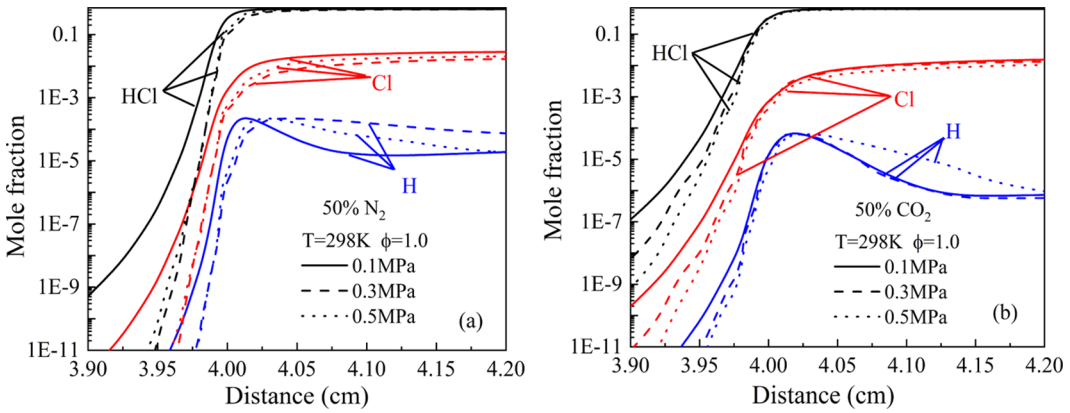

Figure 13. Calculated mole fraction of H, Cl, and HCl under different initial pressures: (a) 50% N_2 and (b) 50% CO_2.

AUTHOR INFORMATION

Corresponding Authors

Guoyan Chen − *School of Mechanical and Power Engineering, Henan Polytechnic University, Jiaozuo 454003, China*; Email: 254568182@qq.com

Weiwei Yu − *State Key Laboratory of Coal Mine Safety Technology, Fushun 113122, China; China Coal Technology & Engineering Group Shenyang Research Institute, Fushun 113122, China*; Email: 463663043@qq.com

Authors

Jianing Chen − *School of Mechanical and Power Engineering, Henan Polytechnic University, Jiaozuo 454003, China*; orcid.org/0000-0002-2765-873X

Anchao Zhang − *School of Mechanical and Power Engineering, Henan Polytechnic University, Jiaozuo 454003, China*; orcid.org/0000-0002-0704-6736

Haoxin Deng − *School of Mechanical and Power Engineering, Henan Polytechnic University, Jiaozuo 454003, China*

Xiaoping Wen − *School of Mechanical and Power Engineering, Henan Polytechnic University, Jiaozuo 454003, China*; orcid.org/0000-0002-5821-5130

Fahui Wang − *School of Mechanical and Power Engineering, Henan Polytechnic University, Jiaozuo 454003, China*

Yanyang Mei − *School of Mechanical and Power Engineering, Henan Polytechnic University, Jiaozuo 454003, China*

Wei Sheng − *School of Mechanical and Power Engineering, Henan Polytechnic University, Jiaozuo 454003, China*

Complete contact information is available at: https://pubs.acs.org/10.1021/acsomega.1c07313

Notes

The authors declare no competing financial interest.

ACKNOWLEDGMENTS

The authors appreciate the support of the Innovative Research Team of Henan Polytechnic University (T2020-3) and the National Natural Science Foundation of China (No. 51774115). The authors thank the editors and reviewers for their careful review and many constructive suggestions on the manuscript.

REFERENCES

(1) Oppelt, E. T. Incineration of hazardous waste. *J. Air Pollut. Control Assoc.* **1987**, *37*, 558−586.

(2) Chelliah, H.; Yu, G.; Hahn, T.; Law, C. K. An experimental and numerical study on the global and detailed kinetics of premixed and nonpremixed flames of chloromethane, methane, oxygen and nitrogen. *Symp. Combust.* **1992**, *24*, 1083−1090.

(3) Wang, H.; Hahn, T.; Sung, C.; Law, C. K. Detailed oxidation kinetics and flame inhibition effects of chloromethane. *Combust. Flame* **1996**, *105*, 291−307.

(4) Leylegian, J.; Zhu, D.; Law, C. K.; Wang, H. Experiments and numerical simulation on the laminar flame speeds of dichloromethane and trichloromethane. *Combust. Flame* **1998**, *114*, 285−293.

(5) Leylegian, J.; Law, C.; Wang, H. Laminar flame speeds and oxidation kinetics of tetrachloromethane. *Symp. Combust.* **1998**, *27*, 529−536.

(6) Schug, K.; Manheimer-Timnat, Y.; Yaccarino, P.; Glassman, I. Sooting behavior of gaseous hydrocarbon diffusion flames and the influence of additives. *Combust. Sci. Technol.* **1980**, *22*, 235−250.
(7) Senkan, S.; Robinson, J.; Gupta, A. Sooting limits of chlorinated hydrocarbon methane-air premixed flames. *Combust. Flame* **1983**, *49*, 305−314.
(8) Slootmaekers, P.; Van Tiggelen, A. Fluorine and chlorine flames. *Bull. Soc. Chim. Belges* **1958**, *67*, 135−146.
(9) Mann, D.; Thrush, B.; Lide, D., Jr.; Ball, J. J.; Acquista, N. Spectroscopy of Fluorine Flames. I. Hydrogen-Fluorine Flame and the Vibration-Rotation Emission Spectrum of HF. *J. Chem. Phys.* **1961**, *34*, 420−431.
(10) Cooley, S. D.; Anderson, R. C. Flame Propagation Studies Using the Hydrogen-Bromine Reaction. *Ind. Eng. Chem.* **1952**, *44*, 1402−1406.
(11) Cooley, S. D.; Lasater, J. A.; Anderson, R. C. Effect of Composition on Burning Velocities in Hydrogen-Bromine Mixtures1. *J. Am. Chem. Soc.* **1952**, *74*, 739−743.
(12) Cooley, S. D.; Anderson, R. C. Burning Velocities in Deuterium-Bromine and Hydrogen-Bromine Mixtures. *J. Am. Chem. Soc.* **1955**, *77*, 235−237.
(13) van Tiggelen, A.; Poncelet, J.; Slootmaekers, P. Eine Beziehung für die Flammengeschwindigkeiten verschiedener Brennstoffgemische. *Z. Elektroch. Ber. Bunsenges. Phys. Chem.* **1957**, *61*, 579−583.
(14) Corbeels, R.; Scheller, K. Observations on the kinetics of hydrogen-chlorine flames. *Symp. Combust.* **1965**, *10*, 65−75.
(15) Leylegian, J.; Sun, H.; Law, C. Laminar flame speeds and kinetic modeling of hydrogen/chlorine combustion. *Combust. Flame* **2005**, *143*, 199−210.
(16) Glarborg, P. Hidden interactions - Trace species governing combustion and emissions. *Proc. Combust. Inst.* **2007**, *31*, 77−98.
(17) Roesler, J.; Yetter, R.; Dryer, F. The Inhibition of the CO/H_2O/O_2 Reaction by Trace Quantities of HCl. *Combust. Sci. Technol.* **1992**, *82*, 87−100.
(18) Roesler, J.; Yetter, R.; Dryer, F. Detailed kinetic modeling of moist CO oxidation inhibited by trace quantities of HCl. *Combust. Sci. Technol.* **1992**, *85*, 1−22.
(19) Roesler, J.; Yetter, R.; Dryer, F. Perturbation of moist CO oxidation by trace quantities of CH_3Cl. *Combust. Sci. Technol.* **1994**, *101*, 199−229.
(20) Roesler, J.; Yetter, R.; Dryer, F. Kinetic interactions of CO, NOx, and HCI emissions in postcombustion gases. *Combust. Flame* **1995**, *100*, 495−504.
(21) Roesler, J.; Yetter, R.; Dryer, F. Inhibition and oxidation characteristics of chloromethanes in reacting CO/H_2O/O_2 mixtures. *Combust. Sci. Technol.* **1996**, *120*, 11−37.
(22) Dixon-Lewis, G.; Marshall, P.; Ruscic, B.; Burcat, A.; Goos, E.; Cuoci, A.; Frassoldati, A.; Faravelli, T.; Glarborg, P. Inhibition of hydrogen oxidation by HBr and Br_2. *Combust. Flame* **2012**, *159*, 528−540.
(23) Howard, J. B.; Kausch, W. J., Jr. Soot control by fuel additives. *Prog. Energy Combust. Sci.* **1980**, *6*, 263−276.
(24) Haynes, B.; Jander, H.; Mätzing, H.; Wagner, H. G. The influence of gaseous additives on the formation of soot in premixed flames. *Symp. Combust.* **1982**, *19*, 1379−1385.
(25) Linak, W. P.; Wendt, J. O. Nitrogen oxide/chlorine interactions in a laboratory swirl flame combustor. *Combust. Sci. Technol.* **1996**, *115*, 69−82.
(26) Linak, W. P.; Wendt, J. O. Trace metal transformation mechanisms during coal combustion. *Fuel Process. Technol.* **1994**, *39*, 173−198.
(27) Miller, B.; Dugwell, D.; Kandiyoti, R. The influence of injected HCl and SO_2 on the behavior of trace elements during wood-bark combustion. *Energy Fuels* **2003**, *17*, 1382−1391.
(28) Mulholland, J.; Sarofim, A.; Beer, J. Chemical effects of fuel chlorine on the envelope flame ignition of droplet streams. *Combust. Sci. Technol.* **1992**, *85*, 405−417.
(29) Rozlovskii, A. Kinetika Temnovoi Reaktsii Khlorovodorodnoi Smesi. 3. Normalnoe Gorenie Khlorovodorodnykh Smesei. *Zh. Fiz. Khim.* **1956**, *30*, 2489−2498.
(30) Law, C.; Sung, C. Structure, aerodynamics, and geometry of premixed flamelets. *Prog. Energy Combust. Sci.* **2000**, *26*, 459−505.
(31) Ren, X.; Sun, R.; Chi, H.-H.; Meng, X.; Li, Y.; Levendis, Y. A. Hydrogen chloride emissions from combustion of raw and torrefied biomass. *Fuel* **2017**, *200*, 37−46.
(32) Tillman, D. A.; Duong, D.; Miller, B. Chlorine in Solid Fuels Fired in Pulverized Fuel Boilers-Sources, Forms, Reactions, and Consequences: A Literature Review. *Energy Fuels* **2009**, *23*, 3379−3391.
(33) Giurcan, V.; Mitu, M.; Razus, D.; Oancea, D. Laminar flame propagation in rich ethane-air-inert mixtures. *Rev. Chim.* **2016**, *67*, 1084−1089.
(34) Giurcan, V.; Mitu, M.; Movileanu, C.; Razus, D. Temperature, pressure and dilution effect on laminar burning velocity of propane-air. *Rev. Roum. Chim.* **2016**, *61*, 517−524.
(35) Mitu, M.; Giurcan, V.; Razus, D.; Oancea, D. Inert gas influence on propagation velocity of methane-air laminar flames. *Rev. Chim.* **2018**, *69*, 196−200.
(36) Giurcan, V.; Mitu, M.; Movileanu, C.; Razus, D.; Oancea, D. Influence of inert additives on small-scale closed vessel explosions of propane-air mixtures. *Fire Saf. J.* **2020**, *111*, No. 102939.
(37) Wang, J.; Huang, Z.; Kobayashi, H.; Ogami, Y. Laminar burning velocities and flame characteristics of CO/H_2/CO_2/O_2 mixtures. *Int. J. Hydrogen Energy* **2012**, *37*, 19158−19167.
(38) Lutz, A. E.; Rupley, F. M.; Kee, R. J.; Reynolds, W.; Meeks, E. *EQUIL: A CHEMKIN Implementation of STANJAN for Computing Chemical Equilibria*; Reaction Design Inc., 1998.
(39) Cai, X.; Wang, J.; Zhang, W.; Xie, Y.; Zhang, M.; Huang, Z. Effects of oxygen enrichment on laminar burning velocities and Markstein lengths of CH_4/O_2/N_2 flames at elevated pressures. *Fuel* **2016**, *184*, 466−473.
(40) Qiao, L.; Gan, Y.; Nishiie, T.; Dahm, W. J.; Oran, E. S. Extinction of premixed methane/air flames in microgravity by diluents: Effects of radiation and Lewis number. *Combust. Flame* **2010**, *157*, 1446−1455.
(41) Dandy, D. S. *Transport Properties & Chemical Equilibrium Calculator*; Colorado State University, 2018.
(42) Xiang, L.; Dong, W.; Hu, J.; Nie, X.; Ren, F.; Chu, H. Numerical study on CH_4 laminar premixed flames for combustion characteristics in the oxidant atmospheres of N_2/CO_2/H_2O/Ar-O_2. *J. Energy Inst.* **2020**, *93*, 1278−1287.
(43) Mitu, M.; Giurcan, V.; Razus, D.; Oancea, D. Inert gas influence on the laminar burning velocity of methane-air mixtures. *J. Hazard. Mater.* **2017**, *321*, 440−448.
(44) Law, C. K. *Combustion Physics*; Cambridge University Press, 2010.
(45) Law, C. Propagation, structure, and limit phenomena of laminar flames at elevated pressures. *Combust. Sci. Technol.* **2006**, *178*, 335−360.
(46) Hu, E.; Huang, Z.; He, J.; Miao, H. Experimental and numerical study on laminar burning velocities and flame instabilities of hydrogen−air mixtures at elevated pressures and temperatures. *Int. J. Hydrogen Energy* **2009**, *34*, 8741−8755.
(47) Egolfopoulos, F.; Law, C. Chain mechanisms in the overall reaction orders in laminar flame propagation. *Combust. Flame* **1990**, *80*, 7−16.

https://doi.org/10.1021/acsomega.1c07313
ACS Omega 2022, 7, 7350−7360